

Worldwide alteration of lake mixing regimes in response to climate change

Article

Accepted Version

Woolway, R. I. ORCID: <https://orcid.org/0000-0003-0498-7968>
and Merchant, C. J. ORCID: <https://orcid.org/0000-0003-4687-9850> (2019) Worldwide alteration of lake mixing regimes in response to climate change. *Nature Geoscience*, 12. pp. 271-276. ISSN 1782-0908 doi: <https://doi.org/10.1038/s41561-019-0322-x> Available at <https://centaur.reading.ac.uk/82814/>

It is advisable to refer to the publisher's version if you intend to cite from the work. See [Guidance on citing](#).

To link to this article DOI: <http://dx.doi.org/10.1038/s41561-019-0322-x>

Publisher: Nature

All outputs in CentAUR are protected by Intellectual Property Rights law, including copyright law. Copyright and IPR is retained by the creators or other copyright holders. Terms and conditions for use of this material are defined in the [End User Agreement](#).

www.reading.ac.uk/centaur

CentAUR

Central Archive at the University of Reading

Reading's research outputs online



1 **Title**

2 Worldwide alteration of lake mixing regimes in response to climate change

3

4 **Author information**

5 R. Iestyn Woolway^{1*}, Christopher J. Merchant^{1, 2}

6

7 1. Department of Meteorology, University of Reading, Reading, UK

8 2. National Centre for Earth Observation, University of Reading, Reading, UK

9

10 *now at Dundalk Institute of Technology, Dundalk, Ireland

11

12 **Lakes hold much of Earth's accessible liquid freshwater, support biodiversity and**
13 **provide key ecosystem services to people around the world. However, they are**
14 **vulnerable to climate change, for example through shorter durations of ice cover, or**
15 **through rising lake surface temperatures. Here we use a one-dimensional, numerical**
16 **lake model to assess climate change impacts on mixing regimes in 635 lakes worldwide.**
17 **We run the lake model with input data from four state-of-the-art model projections of**
18 **21st century climate under two emissions scenarios. Under the scenario with higher**
19 **emissions (Representative Concentration Pathway 6.0), many lakes are projected to**
20 **have reduced ice cover; about a quarter of seasonally ice-covered lakes are permanently**
21 **ice-free by 2080-2100. Surface waters are projected to warm, with a median warming**
22 **across lakes of about 2.5°C, and the most extreme warming at about 5.5°C. The**
23 **projections suggest that around 100 of the studied lakes are projected to undergo**
24 **changes in their mixing regimes. About a quarter of these lakes which are currently**
25 **classified as monomictic - that undergo one mixing event in most years - will become**
26 **permanently stratified systems. About a sixth of these which are currently dimictic -**
27 **that mix twice per year - will become monomictic. We conclude that many lakes will**
28 **mix less frequently in response to climate change.**

29

30 Documented climate-related changes in lakes include shorter durations of winter ice
31 cover¹⁻⁴ and higher lake surface temperatures⁵⁻⁹. Recent global studies of lake surface
32 temperature trends show that many lakes, predominantly those that experience seasonal ice
33 cover, are warming at rates in excess of ambient air temperature⁷⁻⁸. Studies of lake
34 temperature responses to climate change have improved our understanding of the
35 consequences of warming on lake ecosystems^{10, 11}. Here, we assess for 635 globally
36 distributed large lakes how projected climate trends are likely to change lake stratification
37 and mixing. Because these aspects of lake dynamics exert significant control on nutrient
38 fluxes, oxygenation and biogeochemical cycling^{12, 13}, considering stratification and mixing is
39 critical for anticipating the repercussions of temperature change throughout lake
40 environments and associated ecosystems.

41

42 **Stratification and mixing regimes in lakes**

43 Thermal stratification occurs in lakes as a result of the thermal-expansion properties of water.
44 The time evolution of stratification is determined by the balance between turbulence, which
45 acts to enhance mixing, and buoyancy forces, which act to suppress turbulence and result in a

46 vertical layering¹⁴. The vertical layering that exists during stratification exerts strong control
47 on the transport of nutrients and oxygen between the surface and deep water of lakes and the
48 vertical distribution and composition of lake biota. Lakes that are permanently mixed
49 (continuous cold/warm polymictic) or those that mix frequently (discontinuous cold/warm
50 polymictic) differ markedly in their physical, chemical and biological functioning from lakes
51 that are stratified permanently (meromictic) or semi-permanently (oligomictic, characterised
52 by variable temporal periods of incomplete mixing, interspersed with occasional mixing)^{14, 15}.
53 Lakes that stratify seasonally can be classed as dimictic if they have two stratification
54 seasons, or monomictic (cold or warm) if they stratify only once per year (see Methods; Fig.
55 S1). Seasonal mixing serves as a basis for lake regime classification¹⁶ and as a necessary
56 component of projecting how lake ecosystems will respond to climate change.

57

58 The mixing class to which a lake belongs depends primarily on (i) whether or not it
59 experiences ice cover annually, and (ii) the number of times during a year in which it
60 stratifies continuously (Fig. S1). Ice-covered lakes tend to occur in less-maritime, high-
61 latitude and high-elevation regions (Fig. 1A). Satellite observations of 635 lakes from 1995 to
62 2011 (Table S1), ~50% of which experienced ice cover annually, illustrate that the
63 climatological duration of ice cover varies systematically with mean air temperature (Fig. 1B;
64 produced using air temperature from the ERA-Interim reanalysis¹⁷). With regards to the
65 stratification criterion for mixing class, surface water temperature observations can be used to
66 distinguish between dimictic and monomictic (cold or warm) lakes (Fig. 1C, 1D): in warm
67 monomictic lakes, surface water temperature does not cool below 4°C (near the maximum
68 density of freshwater), while in cold monomictic lakes, surface water temperature does not
69 warm above 4°C. No lake surface water temperature threshold separates thermally stratifying
70 and polymictic lakes, as other factors can have a substantial influence, notably lake depth
71 (e.g., shallow lakes can mix easily). The global heterogeneity of lake sizes and depths^{18, 19}
72 suggests that lake-mixing classes should be heterogeneously distributed.

73

74 **Global patterns of lake mixing regimes**

75 In this study, we assess the contemporary mixing class of 635 lakes worldwide, by
76 developing a classification scheme applied to numerical simulation results from a lake model,
77 and then use this model to project future mixing classes under climate change scenarios. This
78 approach enables meromictic, oligomictic, monomictic, dimictic and polymictic mixing
79 classes to be determined.

80

81 To assess the contemporary mixing classes, we first optimise key parameters of the
82 lake model, FLake^{20, 21}, to represent the dynamics of each individual lake. The optimisation
83 constrains the model to represent observed lake surface water temperature time series (see
84 Methods). The ability of the optimised lake model to represent a wide range of lake dynamics
85 is evaluated by comparing simulations with independent temperature observations, ice cover
86 and lake mixing regimes under historic climate conditions. Good agreement is obtained (Fig.
87 S2-S7). Particularly relevant to multi-decadal projection is that the lake model is able to
88 simulate accurately historic multi-decadal variations in lake temperature back to the start of
89 the 20th century (Fig. S4) and to identify successfully the mixing regime of 72% of lakes for
90 which independent mixing regime classifications were found (Fig. S7; Table S2). Up to 85%

91 of inter-decadal variability in lake surface temperature is explained by the lake model forced
92 with representations of historic climate conditions.

93
94 The identified lake mixing regimes demonstrate a diverse array of mixing types (Fig.
95 1E-1F). Dimictic lakes are most common in our global dataset (Fig. S8), a result of the
96 majority of our study lakes being relatively large (all studies lakes exceed 27 km² in area) and
97 situated north of 40°N, where the global lake abundance is highest¹⁸. The proportion of
98 dimictic and polymictic lakes is large in north temperate latitudes, as expected, and
99 meromictic lakes are common in the tropics (Fig. 1E-1F).

100 **Climate-related changes in lake mixing regimes**

101 To project future changes in mixing class, the lake model is forced by four climate
102 projections available from the Inter-Sectoral Impact Model Intercomparison Project²²,
103 namely, HadGEM2-ES, GFDL-ESM2M, IPSL-CM5A-LR and MIROC5 (see Methods for
104 details), under two Representative Concentration Pathway (RCP) scenarios. The main figures
105 presented here show the results from the lake model forced with bias-corrected HadGEM2-
106 ES projections. To indicate the uncertainty of projections, we show or quote the spread of
107 results from the lake model across all four climate model projections. Changes projected for
108 2080-2100 are quoted relative to the period 1985-2005.

109
110
111 The responses of lake mixing regimes to climate change are complex and may not be
112 associated closely with change in any one climatic variable. Rather, the mixing regime of a
113 lake will depend on changes in a combination of climatic factors that contribute to the lake
114 heat budget (e.g., air temperature, solar and thermal radiation, cloud cover, wind speed,
115 humidity). Under future scenarios RCP 2.6 and 6.0, we project that the number of annual ice-
116 covered days will decrease substantially (Fig. 2A, 2B) by 2080-2100. For RCP 2.6, the
117 decrease is on average (across all lakes that are seasonally ice covered during the historic
118 period) 15 days, the standard deviation of this mean change across the four-member ensemble
119 being 5 days. For RCP 6.0, the projected mean change is -29 ± 8 days. In the most extreme
120 cases under RCP 6.0, the projected decreases of ice-covered days exceed 60 days. The
121 simulations project that $24\pm 5\%$ of lakes that display winter ice cover in the historic period
122 will be ice-free by the end of the 21st century under the RCP 6.0 scenario. The increase in
123 annual mean lake surface temperature is projected to be $1.1\pm 0.4^{\circ}\text{C}$ and $2.3\pm 0.6^{\circ}\text{C}$ under RCP
124 2.0 and 6.0, respectively (Fig. 2C, 2D), by 2080-2100. For individual lakes, projected
125 warming can be higher, the largest projected increase being $5.4\pm 1.1^{\circ}\text{C}$ under RCP 6.0.
126 $99\pm 0.5\%$ of lakes are projected to increase in mean temperature under RCP 2.6, and all
127 ($100\pm 0\%$) increase under RCP 6.0.

128
129 Decreases in winter ice cover and increases in lake surface temperatures would be
130 expected qualitatively to modify the distribution of lake mixing regimes. Next, we investigate
131 the global extent and magnitude of response in the projections to quantify this expectation.
132 The projections suggest that alterations in lake mixing regimes will occur during the 21st
133 century (Fig. 3, Fig. S9-S10). Specifically, in the projections under RCP 2.6 and 6.0,
134 respectively, 59 ± 7 and 96 ± 15 lakes change mixing class.

136 The most common identified alteration in mixing class ($25\pm 5\%$ of altered lakes under
137 RCP 6.0) is a change from warm monomictic to meromictic. This means that a significant
138 minority of lakes that do not currently experience ice cover and stratify once annually are
139 projected to become permanently stratified systems by the end of the 21st century. In addition,
140 all of the lakes identified as being oligomictic during the historic period transition to the
141 meromictic class by 2080-2100. A lack of vertical mixing by the end of the 21st century will
142 result in reduced upwelling of nutrients from deep to shallow waters and a decrease in deep-
143 water oxygen concentrations, which can lead to reduced lake productivity¹⁰ and the formation
144 of deep-water dead zones¹², respectively. Oxygen depletion at depth can be detrimental to the
145 habitat for fish²³ and can modify biogeochemical processes resulting in, for example, the
146 potential release of phosphorus and ammonium into the water column²⁴ and the production of
147 potentially toxic metal ions²⁵.

148
149 The second most common identified alteration in mixing class (across the model
150 ensemble) is a change from dimictic to warm monomictic ($17\pm 5\%$ of altered lakes under
151 RCP 6.0) (Fig. 3, Fig. S9-S10). This alteration occurs when lakes that were historically ice
152 covered no longer freeze in winter but still stratify during summer. The projected absence of
153 winter ice has implications for those lake ecosystems including, among other things, changes
154 in water quality²⁶ and the production and biodiversity of phytoplankton²⁷.

155
156 A very small number of altered lakes are projected to experience fewer continuous
157 periods of stratification, and, as a result, to transition from being categorized as dimictic to
158 polymictic. Such an increase in mixing can be a result of changes in any of the
159 meteorological drivers acting at the lake surface. Short-term variations in surface wind speed,
160 for example, can play an important role in lake stratification and mixing, and could nudge
161 some lakes to a different mixing regime²⁸. The influence of changes in wind speed will,
162 however, be expected to have the most pronounced effects on the mixing regime of shallow
163 lakes. All the lakes that are projected to undergo an increase in the number of mixing events
164 per year are among the shallowest 1% of the lakes studied. Other factors that were not
165 considered in this study may also be important for mixing regime alterations in specific lakes,
166 such as groundwater inputs²⁹, increased inflow of cold water from retreating glaciers³⁰,
167 thermal pollution from nuclear plants³¹, and changes in the magnitude of influent water³²,
168 which will be particularly important for lakes with short residence times or extensive lake
169 level variations³³. Changes in lake transparency can also influence the mixing regime of
170 lakes³⁴, but it is not expected to be a dominant driver of mixing regime alterations in large
171 lakes, such as those included in this study. The influence of transparency on lake mixing and
172 stratification has been shown to decrease with increasing lake size^{35, 36} and the vertical
173 thermal structure will be constrained strongly by fetch³⁷. Thus, transparency is expected to
174 have a greater influence on the vertical thermal structure of relatively small lakes compared
175 to larger ones, as investigated in this study.

176
177 There is scattered evidence of mixing regime alterations already taking place, and
178 ecological consequences of these changes are starting to appear^{38, 39}. Our projections of future
179 lake-mixing regime alterations span a wide range of locations, sizes, and climatic contexts,
180 and suggest a complex pattern of lake responses to climate change. The geographical

181 distribution of lake mixing regime alterations is heterogeneous, because climatic conditions
182 interact with lake-specific contexts, particularly geomorphology. The projections do not
183 support simple expectations of regional consistency in lake responses whereby lakes in a
184 given region will change similarly. Changes in lake temperature will not always translate to
185 changes in lake mixing regimes: some of the lakes which are projected to experience the
186 highest surface warming are not projected to undergo a change in their mixing class. Most
187 lakes that are projected to alter in their mixing regimes currently display anomalous mixing
188 behaviour relative to their dominant mixing classification in some years. Specifically, two-
189 thirds of lakes that are projected to experience an alteration in their mixing regimes had at
190 least three years of anomalous mixing regime during the period 1985 to 2005. Lakes that are
191 currently classified as warm monomictic but fail to mix fully during some winters presently
192 account for 60% of those that are projected to become meromictic (i.e., permanently
193 stratified) in the future. Lakes that are currently seasonally ice-covered and are classified as
194 dimictic but also experience some ice-free winters are projected to become predominantly
195 monomictic by the end of the 21st century. Thus, the projections confirm the intuition that
196 those lakes that currently exhibit anomalous years relative to their usual mixing class are
197 more likely to transition to a different mixing regime in the future.

198

199 **References**

- 200 1. Sharma, S., et al. Widespread loss of lake ice around the Northern Hemisphere in a
201 warming world, *Nature Climate Change* (In press).
- 202 2. Magnuson, J. J. et al. Historical trends in lake and river ice cover in the Northern
203 Hemisphere. *Science* **289**, 1743-1746 (2000).
- 204 3. Fang, X., & Stefan, H. G. Simulations of climate effects on water temperature, dissolved
205 oxygen, and ice and snow covers in lakes of the contiguous U. S. under past and future
206 climate scenarios. *Limnol. Oceanogr.* **54**, 2359-2370 (2009).
- 207 4. Magee, M. R., Wu, C. H., Robertson, D. M., Lathrop, R. C. & Hamilton, D. P. Trends
208 and abrupt changes in 104 years of ice cover and water temperature in a dimictic lake in
209 response to air temperature, wind speed, and water clarity drivers. *Hydrol. Earth Syst.*
210 *Sci.* **20**, 1681-1702 (2016)
- 211 5. Schneider, P., Hook, S. J. Space observations of inland water bodies show rapid surface
212 warming since 1985, *Geophys. Res. Lett.* **37**, doi:10.1029/2010GL045059
- 213 6. Magee, M. R. & Wu, C. H. Response of water temperatures and stratification to changing
214 climate in three lakes with different morphometry. *Hydrol. Earth Syst. Sci.* **21**, 6253-
215 6274 (2017).
- 216 7. O'Reilly, C. et al. Rapid and highly variable warming of lake surface waters around the
217 globe. *Geophys. Res. Lett.* **42**, 10773-10781 (2015).
- 218 8. Austin, J. A., S. M. Colman. Lake Superior summer water temperatures are increasing
219 more rapidly than regional temperatures: A positive ice-albedo feedback. *Geophys. Res.*
220 *Lett.* **34**, doi:10.1029/2006GL029021. (2007).
- 221 9. Livingstone, D. M. Impact of secular climate change on the thermal structure of a large
222 temperate central European lake. *Clim. Change* **57**, 205-225 (2003).
- 223 10. O'Reilly, C. et al. Climate change decreases aquatic ecosystem productivity of Lake
224 Tanganyika, Africa. *Nature* **424**, 766-768 (2003).
- 225 11. O'Beirne, M. D. et al. Anthropogenic climate change has altered primary productivity in
226 Lake Superior. *Nat. Commun.* **8**, 15713 (2017).

- 227 12. North, R. P. et al. Long-term changes in hypoxia and soluble reactive phosphorus in the
 228 hypolimnion of a large temperate lake: consequences of a climate regime shift. *Glob.*
 229 *Change Biol.* **20**, 811-823 (2014).
- 230 13. Yankova, Y., Neuenschwander, S., Köster, O. & Posch, T. Abrupt stop of deep water
 231 turnover with lake warming: Drastic consequences for algal primary producers. *Sci. Rep.*
 232 **7**, 13770 (2017).
- 233 14. Boehrer, B. & Schultze, M. Stratification of lakes. *Rev. Geophys.* **46**, RG2005 (2008).
- 234 15. Boehrer, B., von Rohden, C. & Schultze, M. *Physical Features of Meromictic Lakes:*
 235 *Stratification and Circulation.* In: Gulati, R., Zadereev, E., Degermendzhi, A. (eds)
 236 *Ecology of Meromictic Lakes. Ecological Studies (Analysis and Synthesis)*, **228**,
 237 (Springer, Cham, 2017).
- 238 16. Lewis, W. M., Jr. A revised classification of lakes based on mixing. *Can. J. Fish. Aquat.*
 239 *Sci.* **40**, 1779-1787 (1983).
- 240 17. Dee, D. P. et al. The ERA-Interim reanalysis: configuration and performance of the data
 241 assimilation system. *Q. J. R. Meteorol. Soc.* **137**, 553-597 (2011).
- 242 18. Verpoorter, C. et al. A global inventory of lakes based on high-resolution satellite
 243 imagery. *Geophys. Res. Lett.* **41**, 6396-6402 (2014).
- 244 19. Messenger, M. L. et al. Estimating the volume and age of water stored in global lakes
 245 using a geo-statistical approach. *Nat. Commun.* **7**, 13603 (2016).
- 246 20. Mironov, D. Parameterization of lakes in numerical weather prediction: Part 1.
 247 Description of a lake mode. COSMO Technical Report, No. 11, Deutscher Wetterdienst,
 248 Offenbach am Main, Germany, (2008).
- 249 21. Mironov, D. et al. Implementation of the lake parameterisation scheme FLake into the
 250 numerical weather prediction model COSMO. *Boreal Environ. Res.* **15**, 218–230 (2010).
- 251 22. Frieler, K. et al. Assessing the impacts of 1.5°C global warming - simulation protocol of
 252 the Inter-Sectoral Impact Model Intercomparison Project (ISIMIP2b). *Geosci. Model*
 253 *Dev.* **10**, 4321-4345 (2017).
- 254 23. Regier, H. A., Holmes, J. A. & Pauly, D. Influence of temperature changes on aquatic
 255 ecosystems: an interpretation of empirical data. *Trans. Am. Fish. Soc.* **119**, 374–389
 256 (1990).
- 257 24. Mortimer, C. H. The exchange of dissolved substances between mud and water in lakes,
 258 *J. Ecol.* **29**, 280-329 (1941).
- 259 25. Davison, W. Supply of iron and manganese to an anoxic lake basin, *Nature* **290**, 241-243
 260 (1981).
- 261 26. Weyhenmeyer, G. A., Westöo, A.-K. & Willén, E. Increasingly ice-free winters and their
 262 effects on water quality in Sweden's largest lakes. *Hydrobiologia* **599**, 111-118 (2008).
- 263 27. Weyhenmeyer, G. A., Bleckner, T. & Petterson, K. Changes of the plankton spring
 264 outburst related to the North Atlantic Oscillation. *Limnol. Oceanogr.* **44**, 1788-1792
 265 (1999).
- 266 28. Woolway, R. I., Meinson, P., Nöges, P., Jones, I. D. & Laas, A. Atmospheric stilling
 267 leads to prolonged thermal stratification in a large shallow polymictic lake. *Clim.*
 268 *Change*, **141**, 759-773 (2017).
- 269 29. Rosenberry, D O. et al. Groundwater – the disregarded component in lake water and
 270 nutrient budgets. Part 1: effects of groundwater on hydrology. *Hydrol. Process.* **29**, 2895-
 271 2921 (2015).

- 272 30. Peter, H., & Sommaruga, R. Alpine glacier-fed turbid lakes are discontinuous cold
273 polymictic rather than dimictic. *Inland Waters* **7**, 45-54 (2017).
- 274 31. Kirillin, G., Shatwell, T. & Kasprzak, R. Consequences of thermal pollution from a
275 nuclear plant on lake temperature and mixing regime. *J. Hydrol.* **496**, 47-56 (2013).
- 276 32. Valerio, G., Pilotti, M., Barontini, S. & Leoni, B. Sensitivity of the multiannual thermal
277 dynamics of a deep pre-alpine lake to climatic change. *Hydrol. Processes* **29**, 767-779
278 (2015).
- 279 33. Rimmer, A., Gal, G., Opher, T., Lechinsky, Y. & Yacobi, Y. Z. Mechanisms of long-
280 term variations in the thermal structure of a warm lake. *Limnol. Oceanogr.* **56**, 974-988
281 (2011).
- 282 34. Shatwell, T., Adrian, R. & Kirillin, G. Planktonic events may cause polymictic-dimictic
283 regime shifts in temperate lakes. *Sci. Rep.* **6**, 24361(2016).
- 284 35. Fee, E. J., Hecky, R. E., Kasian, S. E. M. & Cruikshank, D. R. Effects of lake size, water
285 clarity, and climatic variability on mixing depths in Canadian Shield lakes. *Limnol.*
286 *Oceanogr.* **41**, 912-920 (1996).
- 287 36. Read, J. S. & Rose, K. C. Physical responses of small temperate lakes to variation in
288 dissolved organic carbon concentrations. *Limnol. Oceanogr.* **58**, 921-931 (2013).
- 289 37. Gorham, E. & Boyce, F. M. Influence of lake surface area and depth upon thermal
290 stratification and the depth of the summer thermocline. *J. Great Lakes Res.* **15**, 233-245
291 (1989).
- 292 38. Kainz, M. J., Ptacnik, R., Rasconi, S. & Hager, H. H. Irregular changes in lake surface
293 water temperature and ice cover in subalpine Lake Lunz, Austria. *Inland Waters* **7**, 27-33
294 (2017).
- 295 39. Ficker, H., Luger, M. & Gassner, H. From dimictic to monomictic: Empirical evidence of
296 thermal regime transitions in three deep alpine lakes in Austria induced by climate
297 change. *Freshwater Biol.* **62**, 1335-1345 (2017).

298

299 **Acknowledgements**

300 This analysis was funded by EUSTACE (EU Surface Temperature for All Corners of Earth)
301 which has received funding from the European Union's Horizon 2020 Programme for
302 Research and Innovation, under Grant Agreement no 640171. The authors also acknowledge
303 the European Space Agency funding of the ARC-Lake project. We thank Martin Dokulil for
304 providing lake temperature data for Mondsee and Wörthersee. RIW received funding from a
305 European Union's Marie Skłodowska-Curie Individual Fellowship (#791812; INTEL
306 project). This work benefited from participation in the Global Lake Ecological Observatory
307 Network (GLEON).

308

309 **Author Contributions**

310 Both authors developed the concept of the study, designed the analytical experiments,
311 interpreted the results and wrote the paper.

312

313 **Financial and non-financial competing interests**

314 The authors do not have any competing financial or non-financial interests to declare.

315 **Figure captions**

316

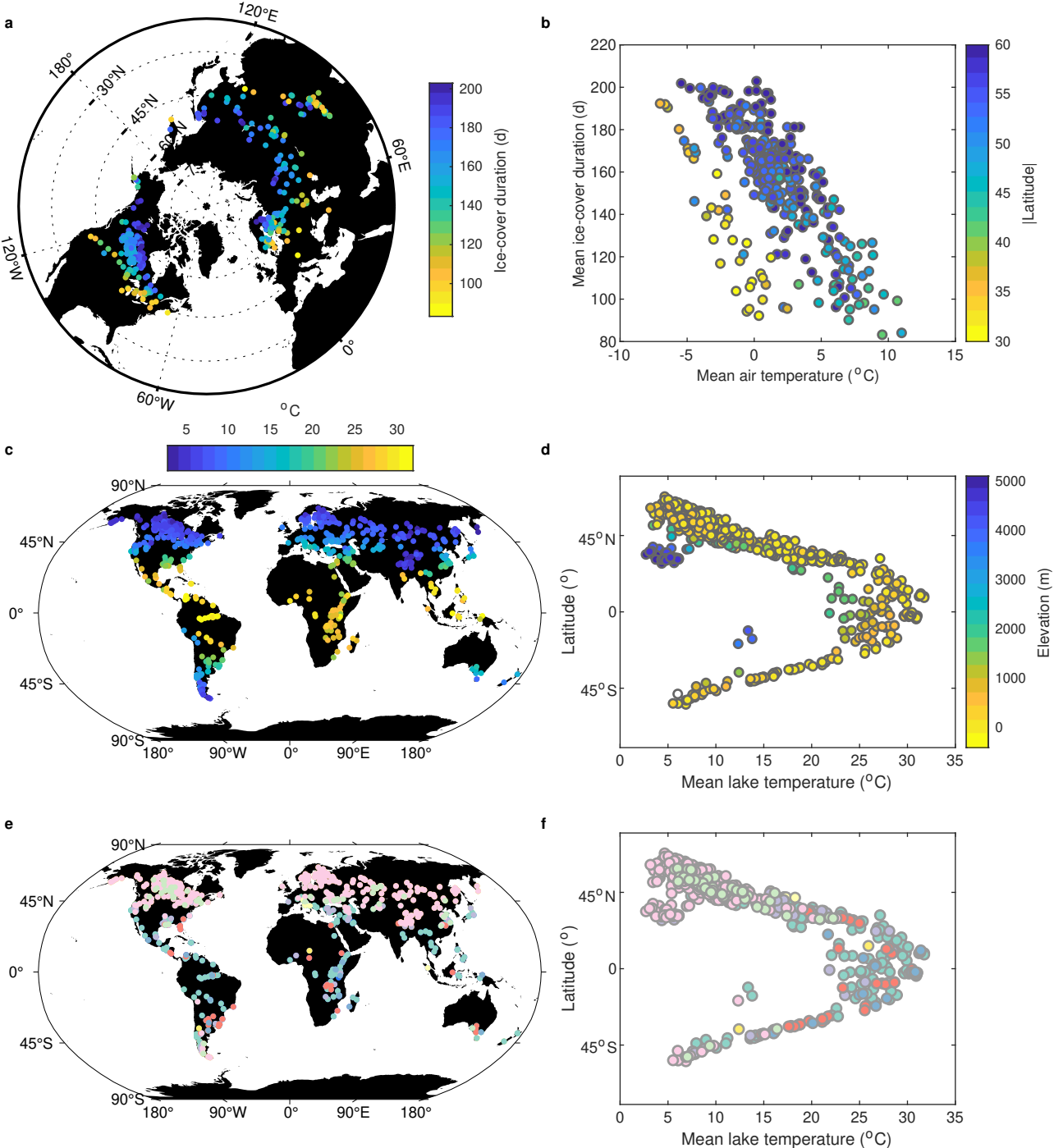
317 **Figure 1. Global patterns in annual mean (1995-2005) ice cover duration, lake surface**
318 **temperature and lake mixing regimes.** (a) Satellite-derived ice cover duration and (b) their
319 relationship with air temperature (from ERA-Interim¹⁷). (c) Global variations in satellite-
320 derived lake surface water temperature and (d) their relationship with latitude and elevation.
321 (e) Global variations in modelled lake mixing regimes and (f) their relationship with latitude
322 and lake surface water temperature. Mixing regimes were identified using the classification
323 scheme of ref. 16, extended to include an oligomictic class, evaluated from a lake model
324 forced by bias-corrected HadGEM2-ES projections. (Lake mixing regimes identified while
325 using bias-corrected projections from other climate models are shown in Fig. S8).

326

327 **Figure 2. Global changes (2080-2100 relative to 1985-2005) in annually averaged ice**
328 **cover duration and lake surface water temperature.** (a) Changes in ice cover duration
329 under RCP 2.6 and 6.0 (shown only for northern hemisphere lakes) from a lake model forced
330 with bias-corrected HadGEM2-ES projections, and (b) all climate model projections from
331 ISIMIP2b, showing also the kernel density estimates (horizontal widths of coloured areas).
332 Changes are also shown for the annual average lake surface temperature under (c-d) RCP 2.6
333 and (E-F) RCP 6.0, showing results from the lake model forced with HadGEM2-ES
334 projections (c and e) as well as all models (d and f). In Figs 2b, 2d, 2f, the mean and standard
335 deviation is also shown (black).

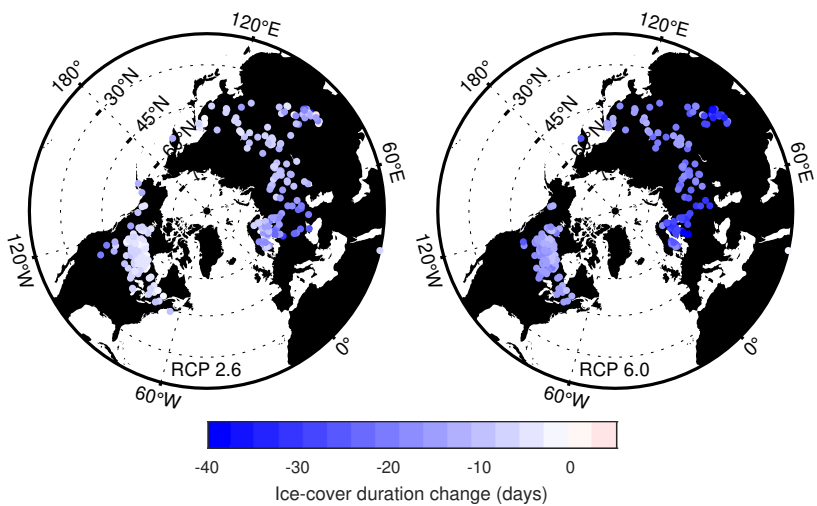
336

337 **Figure 3. Global changes (2080-2100 relative to 1985-2005) in lake mixing regimes.**
338 Shown are climate-related changes in lake mixing regimes under (a) RCP 2.6 and (b) RCP
339 6.0 using a lake model forced with bias-corrected HadGEM2-ES projections (comparison of
340 lake mixing regime alterations identified while using bias-corrected climate projections from
341 other climate models are shown in Figs S9-S10). Every lake that experiences a mixing regime
342 alteration is shown in grey in the maps and the most frequent mixing regime alterations
343 (encompassing 80% of the identified mixing regime shifts) are shown with individual colours
344 (see legend).

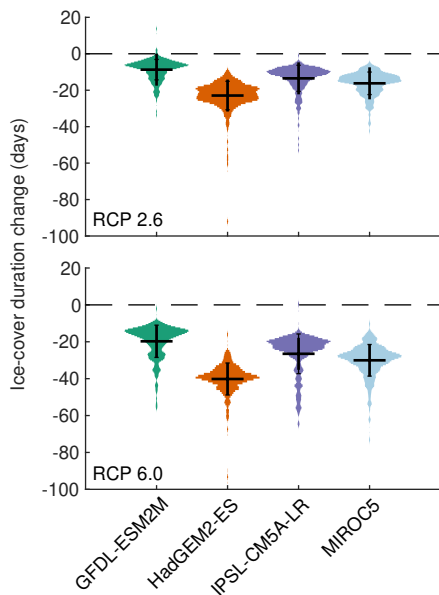


Meromictic	Oligomictic	Warm Monomictic	Disc. Warm Polymictic	Cont. Warm Polymictic
Amictic	Cold Monomictic	Dimictic	Disc. Cold Polymictic	Cont. Cold Polymictic

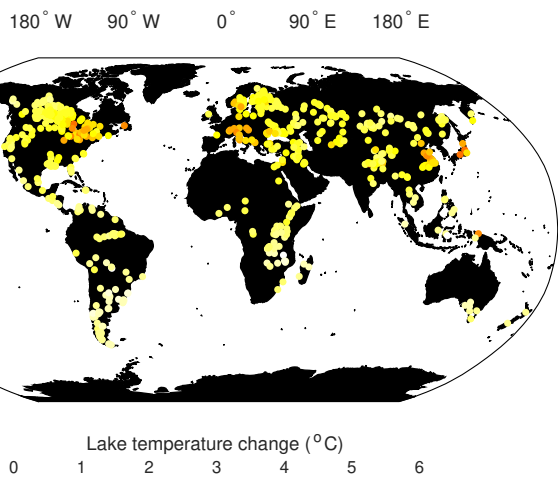
a Projected global change in ice cover and lake temperature



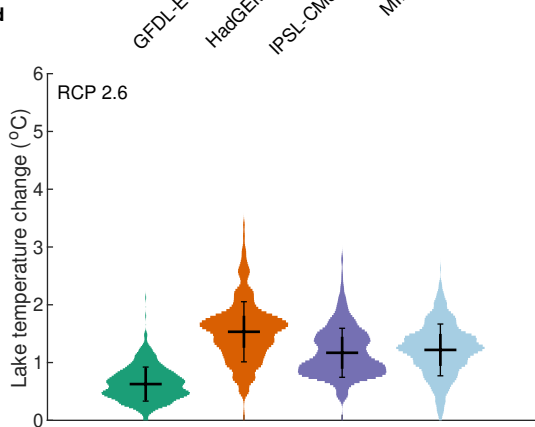
b



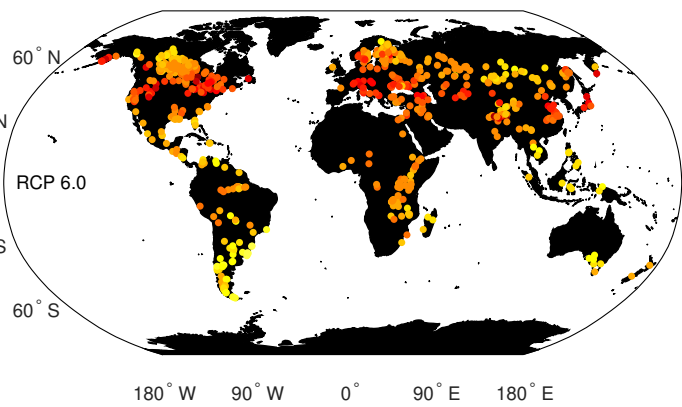
c



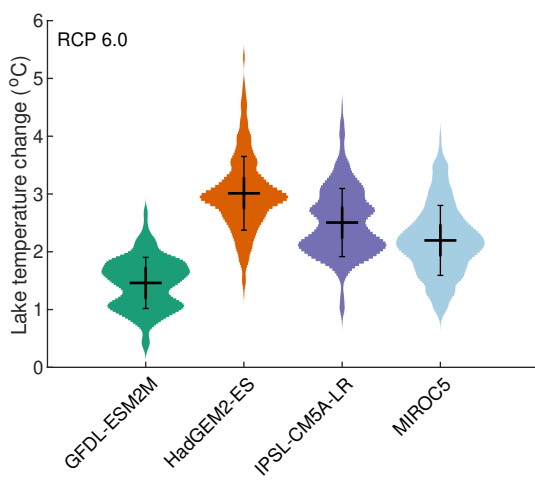
d



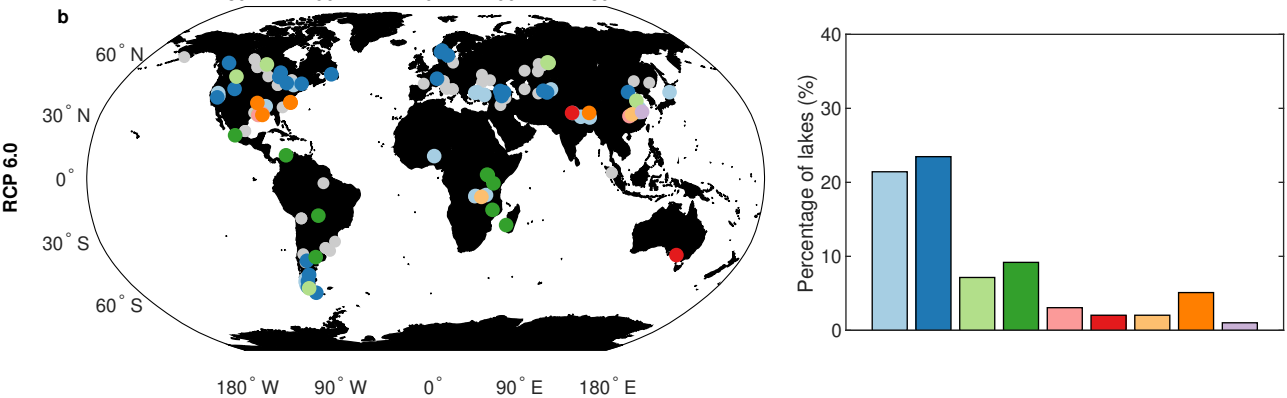
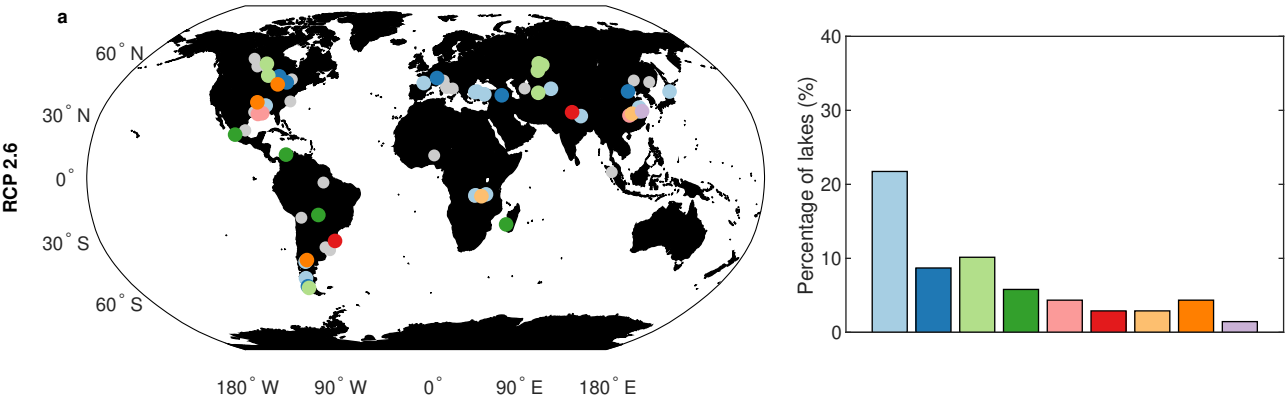
e



f



Projected global mixing regime alterations



Warm Mono. - Meromictic
Dimictic - Warm Mono.
Disc. Cold Poly. - Dimictic

Cont. Warm Poly. - Disc. Warm Poly.
Disc. Col. Poly. - Disc. Warm Poly.
Disc. Warm Poly. - Warm Mono.

Disc. Warm Poly. - Meromictic
Dimictic - Disc. Warm Poly.
Disc. Cold Poly. - Warm Mono.

345 **Methods**

346 Methods, including statements of data availability and any associated references, are
347 available in the online Methods.

348

349 **Online Methods**

350 *Study sites* - The lakes investigated in this study ($n = 635$) vary in their geographic
351 and morphological characteristics (Table S1).

352

353 *Satellite-derived lake temperature and ice cover data* - We utilize lake surface
354 temperatures from the ATSR (Along Track Scanning Radiometer) Reprocessing for Climate:
355 Lake Surface Water Temperature and Ice Cover (ARC-Lake) dataset⁴⁰, available at
356 <http://www.lakemp.net>. In outline, the ARC-Lake surface water temperatures were obtained
357 as follows. Within prescribed lake boundaries a water-detection algorithm using the
358 reflectance channels of the ATSR-2 and AATSR instruments was applied to determine the
359 extent of each lake during the ATSR-2/AATSR period. Within these boundaries, a Bayes'
360 theorem calculation of the probability of clear sky conditions was performed for each image
361 pixel, day and night⁴¹. For pixels with high clear-sky probability, the lake surface water
362 temperature was retrieved from the ATSR-2/AATSR thermal imagery, using an optimal
363 estimation method adapted from radiative-transfer physics-based techniques extensively
364 validated for sea surface temperature⁴². Temperature estimates were gridded and spatio-
365 temporally gap-filled using dynamically interpolating empirical orthogonal functions⁴³. For a
366 fuller account, refer to ref. 40. Daily lake-mean time-series were obtained by averaging
367 across the lake area. Lake-mean surface temperatures are used in order to average across the
368 intra-lake heterogeneity of surface water temperature responses to climate change⁴⁴ and to
369 correspond to the lake-mean model used (see below).

370 The effectiveness of the lake product retrieval algorithms in ARC-Lake has
371 previously been assessed using a dataset of matches to in situ temperature data, consisting of
372 52 observation locations covering 16 lakes and >5,500 individual matches⁴⁰. Overall,
373 agreement was -0.2 ± 0.7 K for daytime and -0.1 ± 0.5 K for night-time matches. ARC-Lake
374 data have been independently validated as part of other studies⁴⁵ and used to validate lake
375 simulations^{46, 47}. In this study we use daily averaged LSWTs, calculated as the average of the
376 day and night-time retrievals. To assess from the daily-mean temperature time-series the
377 periods during which a lake was likely partially or wholly ice covered, we follow ref. 48, and
378 characterise this as the period during which the lake-mean surface water temperature is $< 1^\circ\text{C}$.
379 This corresponds closely to presence of lake ice cover from in-situ observations⁴⁸.

380 The ARC-Lake observations were also used to quantify global patterns in mean lake
381 temperatures and as part of the validation (see below) of the modelled surface temperatures
382 and ice cover duration in lakes globally (Fig. S2, Fig. S5).

383

384 *Lake model* - To simulate depth-resolved lake temperatures, as required to identify
385 mixing regimes in lakes, we used the one-dimensional thermodynamic lake model FLake²⁰,
386 ²¹. FLake is a simplified lake model that is in some instances less accurate than other more
387 computationally expensive models⁴⁹, but which can be efficiently coupled with climate
388 models and is useful for evaluating the impact of climate change projections on lakes⁴⁵.
389 FLake is used widely both for research and as a component in numerical weather prediction⁵⁰.

390 ⁵¹. It has been tested extensively in past studies, including detailed validations across a
391 spectrum of lake contexts. FLake has been used previously for validated simulation of the
392 vertical temperature profile as well as changes to the mixing regime of polymictic and
393 dimictic lakes^{34, 52-53}, and has been shown to reproduce accurately bottom water temperatures
394 as well as the depth and seasonality of the upper mixed layer and thermocline in meromictic
395 lakes^{45, 54, 55}. The model has also been used to reproduce past variability in ice cover timing,
396 intensity and duration⁵⁶, and to investigate the thermal response of polymictic, monomictic
397 and lakes to large-scale climatic shifts⁵⁷. The integrated approach implemented in FLake
398 allows a realistic representation of the major physics behind turbulent and diffusive heat
399 exchange in lakes, including a module to describe the vertical temperature structure of the
400 thermally active layer of bottom sediments, as well as its interaction with the water column
401 above. The lakes investigated in this study all have depths <60 m, an established criterion for
402 applicability of the FLake model in global studies^{46, 50}, except that deeper lakes are included
403 for which we had independent validation of the lake model's ability to simulate mixing
404 regime (Table S1).

405 The meteorological variables required to drive FLake are air temperature at 2 m, wind
406 speed at 10 m, surface solar and thermal radiation, and specific humidity. Lake specific
407 parameters must be set to simulate individual lakes optimally in FLake. These parameters
408 comprise fetch (m), which we fix in this study to the square root of lake surface area, lake
409 depth (m), lake ice albedo and the light attenuation coefficient (K_d , m^{-1}).

410 The prognostic variables needed to initialise FLake simulations include (i) mixed
411 layer temperature, (ii) mixed layer depth, (iii) bottom temperature, (iv) mean temperature of
412 the water column, (v) temperature at the ice (if present) upper surface and (vi) ice thickness
413 (if present). In order to initialise the model runs from physically reasonable fields, we
414 initialise runs from a perpetual-year solution for the lake state. To find this solution for the
415 initialisation state, the model parameters are set as follows: mean depth was extracted from
416 the Hydrolakes database¹⁹, which include observational and geo-statistical model estimates of
417 lake depths worldwide; K_d was set to $3 m^{-1}$ (ref. 50); lake ice albedo was set to 0.6 (ref. 21).
418 The perpetual-year solution is obtained by repeating the forcing from a representative year
419 and running FLake until the annual cycle in modelled lake state is stabilised. The forcing data
420 to derive the initialisation conditions are from the ERA-Interim reanalysis product¹⁷,
421 available at a latitude-longitude resolution of 0.75° .

422 To optimize FLake simulations for each lake, we then use the model-tuning algorithm
423 of ref. 58. This approach estimates the model parameters (lake depth, K_d , and ice albedo;
424 Table S1) to reproduce optimally the observed surface temperature dynamics, specifically by
425 minimising the mean square differences between model and ARC-Lake surface water
426 temperature over the satellite period (1995-2011), in simulations initialised from the
427 perpetual year solution described above. The lake-specific parameters for the model are thus
428 set without reference to any in situ data or to the climate model forcing fields used for
429 historical-period simulation and future projections (see below). Note that while the
430 optimisation is based solely on surface temperature, energy budget considerations suggest
431 that there is some calibration of the temperature profile features, such as development of the
432 thermocline depth, that need to be well represented in order for the surface temperature
433 evolution over time to be calibrated successfully. It is a significant strength of the analysis
434 that the FLake model can be optimised using only surface temperatures and then diagnose

435 successfully the mixing classification of many lakes in which this information was
436 independently available (see below).

437

438 *Simulations forced by climate model projections* – To drive FLake and evaluate lake
439 temperature, ice cover, and mixing regime responses to climate change, we use bias-corrected
440 climate model projections from the Inter-Sectoral Impact Model Intercomparison Project
441 (ISIMIP2b), specifically using projections from GFDL-ESM2M, HadGEM2-ES, IPSL-
442 CM5A-LR, and MIROC5 for historic (1911-2005) and future periods (2081-2100) under two
443 scenarios: RCP 2.6 and RCP 6.0. These pathways encompass a range of potential future
444 global radiative forcing from anthropogenic greenhouse gases and aerosols, and results span a
445 range of potential impacts on lake temperature, ice cover, and mixing regimes. Other
446 commonly used RCP scenarios, RCP 4.5 and RCP 8.5, are not included in ISIMIP2b as they
447 were either considered too high for evaluating future climate impacts (RCP 8.5) or to not
448 provide enough span (RCP 4.5).

449 We downloaded the data needed to drive FLake from ISIMIP2b
450 (<https://www.isimip.org/protocol/#isimip2b>), including projections of air temperature at 2 m,
451 wind speed at 10 m, surface solar and thermal radiation, and specific humidity, which were
452 available at a daily time step and at a grid resolution of 0.5°. Time series data were extracted
453 for the grid point situated closest to the centre of each lake, defined as the maximum distance
454 to land, calculated using the distance-to-land dataset of ref. 59.

455 To verify that FLake, driven by the climate model projections, is able to simulate
456 multi-decadal variations in lake surface temperature (and can therefore be informative with
457 respect to future climate change impacts), we compared the FLake simulations from 1915 to
458 2005 with in-situ measurements from two European lakes, Mondsee and Wörthersee. Lake
459 surface temperature data from these lakes were extracted from the yearbooks of the
460 hydrographic service Austria ([https://www.bmlfuw.gv.at/wasser/wasser-
461 oesterreich/wasserkreislauf/hydrographische_daten/jahrbuecher.html](https://www.bmlfuw.gv.at/wasser/wasser-oesterreich/wasserkreislauf/hydrographische_daten/jahrbuecher.html)). Each of the lakes were
462 sampled daily at a depth of ~0.2 m at the lake-level gauging station. This sampling was
463 performed between 08:00 and 10:00 throughout the observational period, thus limiting the
464 inconsistencies introduced by sampling at different times during a diel cycle, which in some
465 lakes can be very large⁶⁰. Lake temperature simulations, using each of the four model
466 projections in ISIMIP2b, show coherence with inter-annual variability on multi-decadal
467 scales (Fig. S4). Further comparisons of this nature on more widespread lakes would give
468 even greater confidence in long-term simulations, but we were unable to source consistent in
469 situ observations of this length for other lakes.

470 Modelled summer average lake surface temperature driven by the climate model data
471 were also compared with in-situ summer-average lake surface temperatures ($n = 19$) from ref.
472 61, including data from Baikal, Lake Biwa, Bodensee, Lake Erie, Sea of Galilee, Lake Garda,
473 Lac Léman, Lake Huron, Lake Michigan, Neusiedler See, Peipsi, Saimaa, Lake Superior,
474 Lake Tahoe, Lake Taihu, Lake Tanganyika, Lake Taupo, Vänern and Vättern (Fig S3).

475 Simulated lake ice cover duration was validated against ARC-Lake estimates (Fig.
476 S5) of ice cover duration using the proxy measure of the sustained $<1^{\circ}\text{C}$ period⁴⁸. The proxy
477 measure of ice cover was also compared with directly observed ice cover duration from the
478 Global Lake and River Ice Phenology Database⁶² (Fig. S6). To illustrate the accuracy of the
479 proxy metric, the observed ice cover duration was also compared against the simulated period

480 of non-zero ice thickness from the FLake model (Fig. S6). We compared the climatological
481 durations of ice cover in model and observations. The latter comparison requires lakes that
482 were available in both the ARC-Lake dataset (and thus were simulated by FLake) as well as
483 in the Global Lake and River Ice Phenology Database for a substantially overlapping time
484 period. Thirteen such lakes were available. The modelled average number of ice-covered
485 days agreed well with those observed (Fig. S6).

486 Climate-related impacts are assessed as the difference in mean lake conditions (e.g.,
487 mean lake temperature, mean number of ice-covered days, and identified mixing regime)
488 between the period 1985-2005 ('historic' period) and 2080-2100 ('future' period).

489
490 *Lake mixing class* - To classify lakes according to their mixing regimes, during both
491 the historic and future periods, we apply the commonly used classification scheme of ref. 16.
492 The terminology of lake mixing regimes is determined by (i) whether a lake experiences ice
493 cover, and (ii) how many times a lake's water column mixes vertically on an annual basis.
494 Lewis produced a flow diagram describing how to identify a lake's mixing regime (Fig. S1).
495 Lewis' classification scheme identifies five main lake mixing types: amictic, polymictic,
496 monomictic, dimictic, and meromictic. In brief, amictic lakes are those that are persistently
497 ice covered; polymictic lakes are those that mix frequently; monomictic lakes experience one
498 vertical mixing event per year, typically in winter when the vertical temperature difference
499 within a lake is close to zero; dimictic lakes experience two mixing events per year, one
500 following the summer stratified period and the other following the inversely stratified winter
501 period; and meromictic lakes are those that are persistently stratified. Polymictic lakes can be
502 divided further into discontinuous or continuous polymictic, the latter representing a lake that
503 mixes daily. Monomictic and dimictic lakes can be separated further into 'cold' or 'warm'
504 lakes depending on whether or not they experience ice cover annually. Lewis' classification
505 scheme, according to the above definitions, identifies nine mixing regime types: meromictic,
506 warm monomictic, discontinuous warm polymictic, continuous warm polymictic, amictic,
507 cold monomictic, dimictic, discontinuous cold polymictic, and continuous cold polymictic
508 (Fig. S1). In addition to the nine mixing regime types identified by ref. 16 we also distinguish
509 oligomictic lakes in the global classification. Oligomictic lakes are those that are persistently
510 stable in most years, yet completely mix in some years.

511 To determine which mixing regime a lake belongs to according to their vertical
512 temperature profiles, we follow ref. 63-65 and characterise a lake as being mixed when the
513 difference (absolute) between its surface temperature and that at depth (i.e., bottom
514 temperature) is less than 1°C. This is evaluated from the modelled lake temperatures (i.e.,
515 depth-resolved) during the historic and future periods. As an example, we would define a
516 dimictic lake as a lake that (i) experiences winter ice cover, (ii) has an ice-free period, (iii)
517 warms above 4°C with regards to its surface temperature and (iv) experiences two mixing
518 periods within a given year (Fig. S1). For each lake, we determine the mixing class for each
519 year, and assign the overall mixing class to be the dominant model mixing class for the
520 historic and future periods. To differentiate oligomictic and meromictic lakes, all years during
521 each historic or future periods are used to assess whether the lake mixes occasionally. Annual
522 mixing classes are generally consistent across a period: 80% of lakes have the same class for
523 >15 of the 20 years of the historic period, for example.

524 To validate the modelled lake mixing regimes during the historic period, as simulated
525 by FLake driven by each ISIMIP2b model run, we compared results with literature-derived
526 descriptions from 85 lakes, including those described by ref. 66-69, and the World Lake
527 Database (Table S2). In these comparisons we did not separate mixing regimes within an
528 individual class. For example, we did not distinguish between cold and warm monimictic and
529 continuous and discontinuous polymictic, as this information was not available frequently in
530 the literature. Lake mixing regimes assessed from the FLake simulations were in agreement
531 with those from these sources in 72% of cases for three of the ISIMIP2b model runs (Fig. S7)
532 and 73% for the other (IPSL-CM5A-LR).

533

534 **Data availability**

535 Satellite lake temperature data are available at <http://www.laketemp.net>. Observed lake
536 surface temperature data are available at
537 <https://portal.lternet.edu/nis/mapbrowse?packageid=knb-lter-ntl.10001.3>. Climate model
538 projections are available at <https://www.isimip.org/protocol/#isimip2b>.

539

540 **Code availability**

541 The lake model source code is available to download from <http://www.flake.igb-berlin.de/>.

542

543 **References only in Methods**

- 544 40. MacCallum, S. N., & Merchant, C. J. Surface water temperature observations of large
545 lakes by optimal estimation. *Can. J. Remote Sens.* **38**, 25–44 (2012).
- 546 41. Merchant, C. J., Harris, A. R., Maturi, E. & MacCallum, S. Probabilistic physically based
547 cloud screening of satellite infrared imagery for operational sea surface temperature
548 retrieval. *Q. J. R. Meteorol. Soc.* **131**, 2735-2755 (2005).
- 549 42. Merchant, C. J., Le Borgne, P., Marsouin, A. & Roquet, H. Optimal estimation of sea
550 surface temperature from split-window observations. *Remote Sens. Environ.* **112**, 2469-
551 2484 (2008).
- 552 43. Alvera-Azcárate, A., Barth, A., Rixen, M. & Beckers, J. M. Reconstruction of incomplete
553 oceanographic data sets using empirical orthogonal functions: application to the Adriatic
554 Sea surface temperature. *Ocean Model.* **9**, 325-346 (2005)
- 555 44. Woolway, R. I. & Merchant, C. J. Intra-lake heterogeneity of lake thermal responses to
556 climate change: A study of large Northern Hemisphere lakes. *J. Geophys. Res.*
557 *Atmospheres* **123**, 3087-3098 (2018)
- 558 45. Thiery, W., et al., The impact of the African Great Lakes on the regional climate. *J.*
559 *Climate* **28**, 4061-4085 (2015).
- 560 46. Le Moigne, P. et al. Impact of lake surface temperatures simulated by the FLake scheme
561 in the CNRM-CM5 climate model. *Tellus A* **68** (2016).
- 562 47. Versegny, D. L. & MacKay, M. D. Offline implementation and evaluation of the
563 Canadian small lake model with the Canadian land surface scheme over Western Canada.
564 *J. Hydrometeorol.* **18**, 1563-1582 (2017).
- 565 48. Layden, A., Merchant, C. J. & MacCallum, S. Global climatology of surface water
566 temperatures of large lakes by remote sensing. *Int. J. Climatol.* **35**, 4464-4479 (2015).
- 567 49. Stepanenko, V. M. et al. First steps of a Lake Model Intercomparison Project: LakeMIP.
568 *Boreal Environ. Res.* **15**, 191–202 (2010).

- 569 50. Balsamo, G. et al. On the contribution of lakes in predicting near-surface temperature in a
570 global weather forecasting model. *Tellus A* **64**, 15829 (2012).
- 571 51. Rooney, G. & Jones, I. D. Coupling the 1-D lake model FLake to the community land-
572 surface model JULES. *Boreal Environ. Res.* **15**, 501-512 (2010)
- 573 52. Kirillin, G. Modeling the impact of global warming on water temperature and seasonal
574 mixing regimes in small temperate lakes. *Boreal Environ. Res.* **15**, 279–293 (2010).
- 575 53. Kirillin, G., Shatwell, T. & Kasprzak, R. Consequences of thermal pollution from a
576 nuclear plant on lake temperature and mixing regime. *J. Hydrol.* **496**, 47-56 (2013).
- 577 54. Thiery, W. et al. Understanding the performance of the FLake model over two African
578 Great Lakes. *Geosci. Model Dev.* **7**, 317-337 (2014).
- 579 55. Thiery, W. et al. Hazardous thunderstorm intensification over Lake Victoria. *Nat.*
580 *Commun.* **7**, 12786 (2016).
- 581 56. Bernhardt, J. et al. Lake ice phenology in Berlin-Brandenburg from 1947-2007:
582 observations and model hindcasts. *Clim. Change* **112**, 791-817 (2012).
- 583 57. Woolway, R. I. et al. Warming of Central European lakes and their response to the
584 1980s climate regime shift. *Clim. Change* **142**, 505-520 (2017)
- 585 58. Layden, A., MacCallum, S. N. & Merchant, C. J. Determining lake surface water
586 temperatures worldwide using a tuned one-dimensional lake model (Flake, v1). *Geosci.*
587 *Model Dev.* **9**, 2167-2189 (2016).
- 588 59. Carrea, L., Embury, O. & Merchant, C. J. Datasets related to in-land water for limnology
589 and remote sensing applications: Distance-to-land, distance-to-water, water-body
590 identifier and lake-centre co-ordinates. *Geosci. Data J.* **2**, 83–97 (2015).
- 591 60. Woolway, R. I. et al. Diel surface temperature range scales with lake size. *PLoS ONE.*
592 **11**, e0152466 (2016).
- 593 61. Sharma, S. et al. A global database of lake surface temperatures collected by in situ and
594 satellite methods from 1985-2009. *Sci. Data* **2**, 150008 (2015).
- 595 62. Benson, B. & Magnuson, J. J. *Global Lake and River Ice Phenology Database, Version*
596 *1*, Boulder, Colorado USA. NSIDC: National Snow and Ice Data Center [15/01/2018]
597 (2000).
- 598 63. Stefan, H. G., Hondzo, M., Fang, X., Eaton, J. G. & McCormick, J. H. Simulated long-
599 term temperature and dissolved oxygen characteristics of lakes in the north-central
600 United States and associated fish habitat limits. *Limnol. Oceanogr.* **41**, 1124-1135
601 (1996).
- 602 64. Read, J. S. et al. Simulating 2368 temperate lakes reveals weak coherence in stratification
603 phenology. *Ecol. Modell.* **291**, 142-150 (2014).
- 604 65. Woolway, R. I., Maberly, S. C., Jones, I. D. & Feuchtmayr, H. A novel method for
605 detecting the onset of thermal stratification in lakes from surface water measurements.
606 *Water Resour. Res.* **50**, 5131-5140 (2014).
- 607 66. Herdendorf, C. E. *Distribution of the world's large lakes*, pp 3-38, in Tilzer, MM,
608 Serruya C, eds. Large Lakes: Ecological Structure and Function (Springer-Verlag, Berlin,
609 1990).
- 610 67. Titze, D. J. & Austin, J. A. Winter thermal structure of Lake Superior. *Limnol. Oceanogr.*
611 **59**, 1336-1348 (2011).
- 612 68. Katsev S., Verburg, P., Llíros, M., Minor, E. C., Kruger, B. R. & Li, J. *Tropical*
613 *Meromictic Lakes: Specifics of Meromixis and Case Studies of Lakes Tanganyika*,

- 614 *Malawi, and Matano*. In: Gulati R., Zadereev E., Degermendzhi A. (eds) Ecology of
615 Meromictic Lakes. Ecological Studies (Analysis and Synthesis) (Springer, Cham, 2017).
616 69. Syarki, M. T. & Tekanova, E. V. Seasonal primary productivity cycle in Lake Onega.
617 *Biology Bulletin* **35**, 536-540 (2008).

Worldwide alteration of lake mixing regimes in response to climate change

R. Iestyn Woolway^{1*}, Christopher J. Merchant^{1,2}

1. Department of Meteorology, University of Reading, Reading, UK
 2. National Centre for Earth Observation, University of Reading, Reading, UK
- *now at Dundalk Institute of Technology, Dundalk, Ireland

Introduction

The supporting information presented here provides more comprehensive details that complement the analyses presented in the main text, allowing a more complete assessment of our findings.

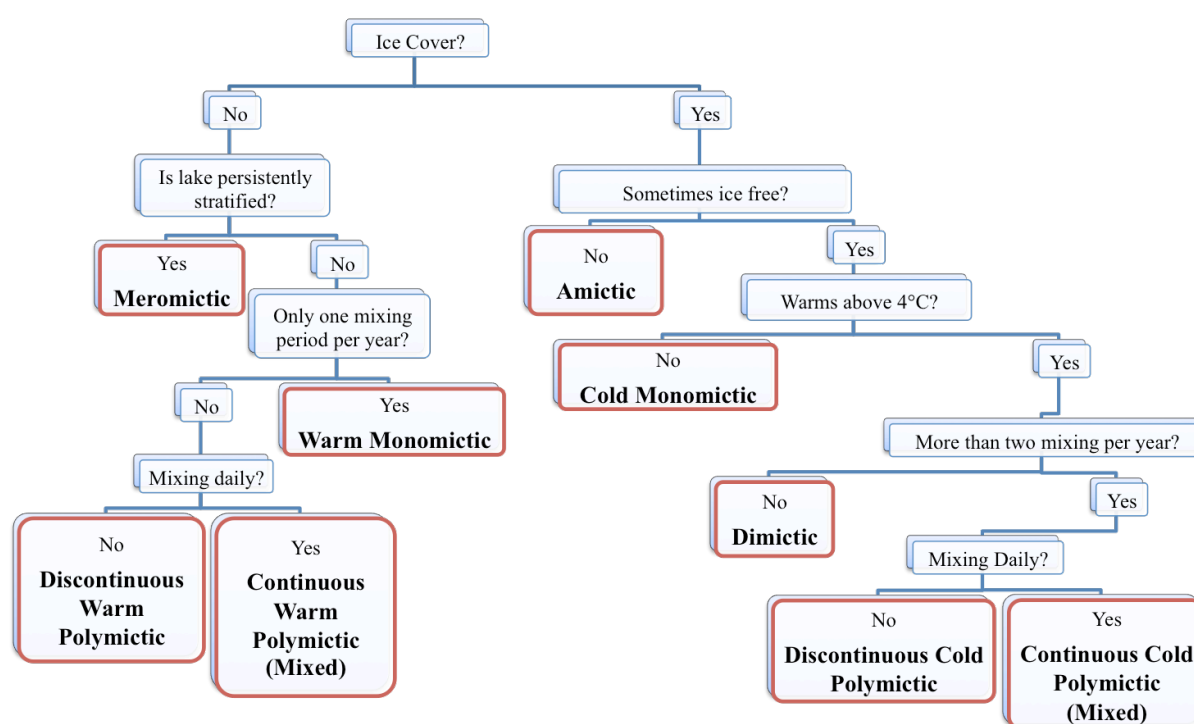


Figure S1. Classification scheme used in this study to determine the mixing regimes of lakes. Modified from ref. 16. The criteria used to define a stratified (or mixed) period is when the top minus bottom (modelled) lake temperature difference (absolute) exceeds (or is lower than) 1°C (see Methods). To assess from the lake surface temperatures (observed or modelled) the period during which a lake is likely ice covered, we follow ref. 48, and characterise this as the period during which the lake-mean surface water temperature is <1°C (see Methods). In addition to the nine mixing regime types identified by ref. 16 we also include oligomictic lakes in the mixing regime classification. Oligomictic lakes are almost persistently stable, mixing only rarely. Specifically, oligomictic lakes do not mix every year but still completely mix in some years.

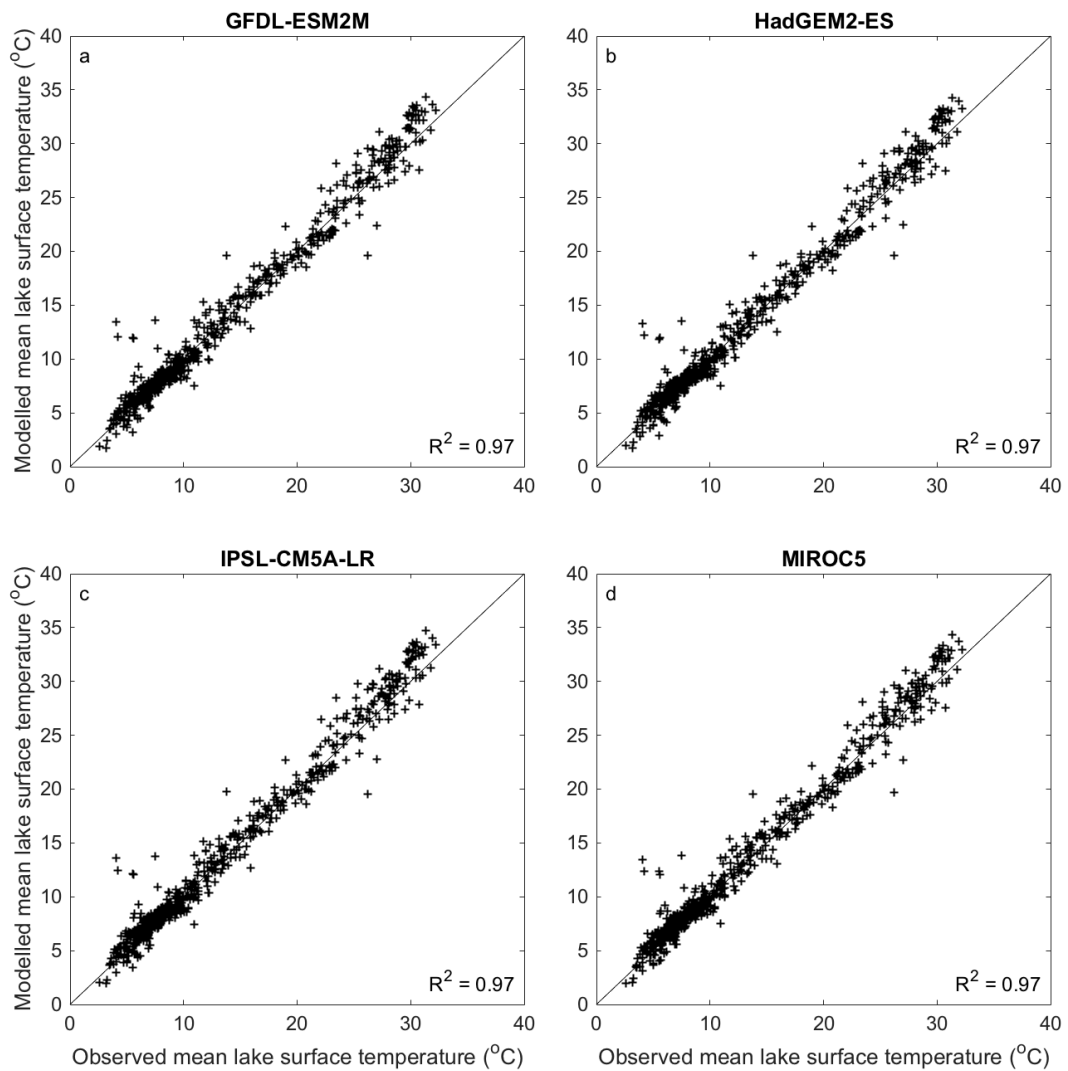


Figure S2. Comparison of annual mean (1995-2005) modelled and observed satellite-derived lake surface water temperatures for 635 lakes in which lake temperature data were available and used in this study. The modelled lake temperatures represent those simulated by a lake model forced with bias-corrected climate projections available from the Inter-Sectoral Impact Model Intercomparison Project, namely (A) GFDL-ESM2M, (B) HadGEM2-ES, (C) IPSL-CM5A-LR and (D) MIROC5. Time series data needed to drive the lake model from each climate projection were extracted for the grid point situated closest to the centre of each lake.

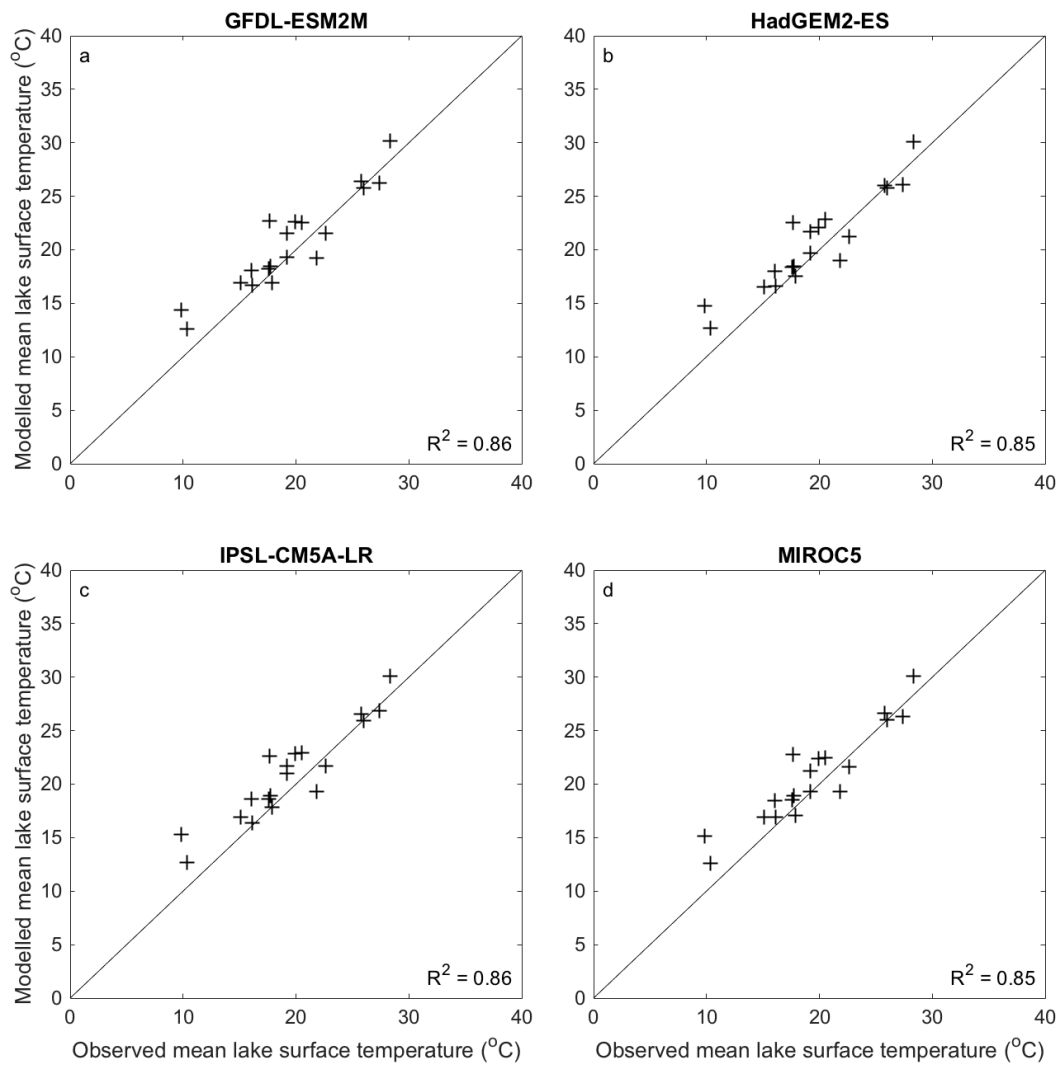


Figure S3. Comparison of summer-average modelled and observed lake surface water temperatures. In-situ summer-average lake surface temperatures are from ref. 61 and include data from Baikal, Lake Biwa, Bodensee, Lake Erie, Sea of Galilee, Lake Garda, Lac Léman, Lake Huron, Lake Michigan, Neusiedler See, Peipsi, Saimaa, Lake Superior, Lake Tahoe, Lake Taihu, Lake Tanganyika, Lake Taupo, Vänern and Vättern. Modelled lake surface temperatures represent those simulated by a lake model forced with bias-corrected climate projections available from the Inter-Sectoral Impact Model Intercomparison Project, namely (A) GFDL-ESM2M, (B) HadGEM2-ES, (C) IPSL-CM5A-LR and (D) MIROC5. Time series data needed to drive the lake model from each climate projection were extracted for the grid point situated closest to the centre of each lake.

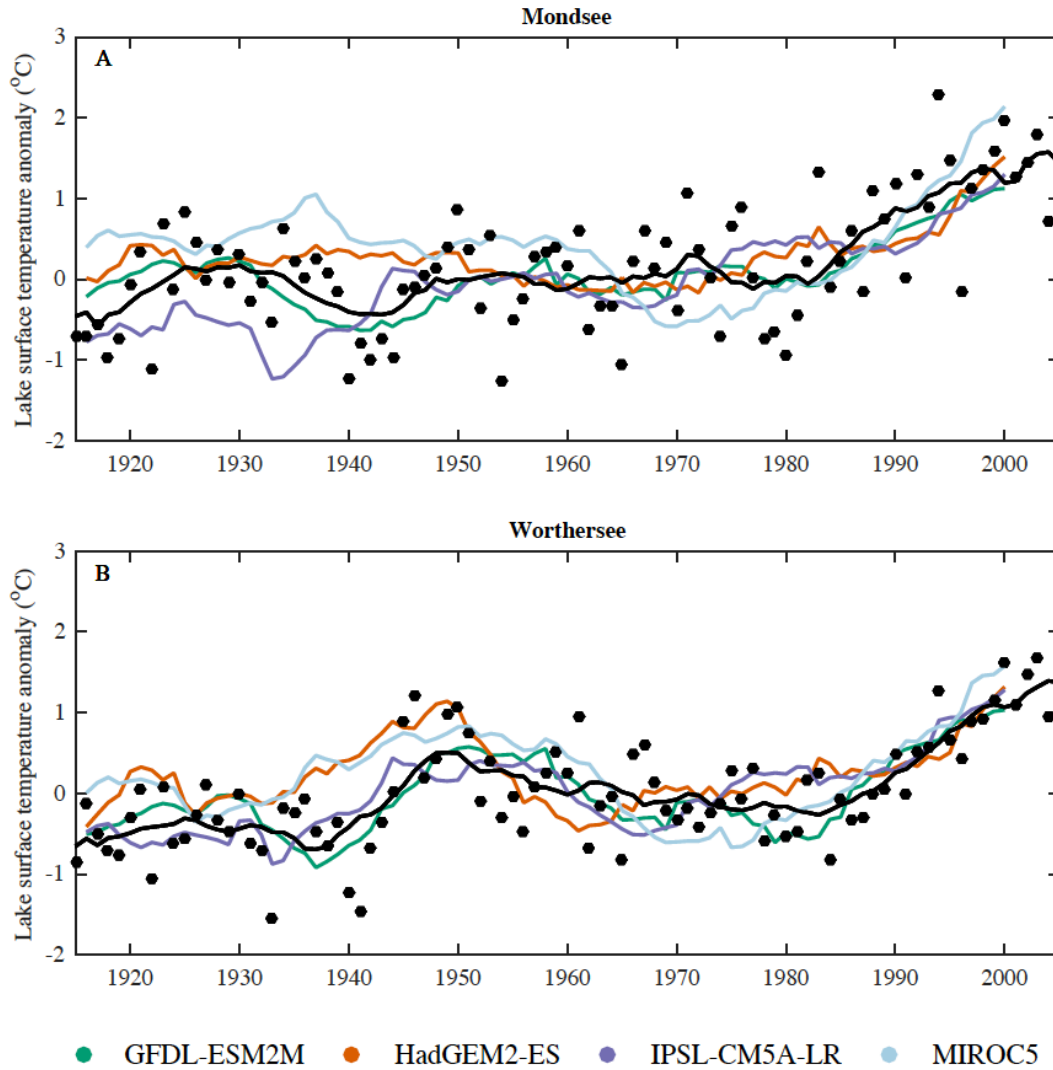


Figure S4. Comparison of observed (black) and modelled (colour) annual mean lake surface temperature anomalies from 1915 to 2005. Modelled lake surface temperatures represent those simulated by a lake model forced with bias-corrected climate projections available from the Inter-Sectoral Impact Model Intercomparison Project, namely, GFDL-ESM2M (green), HadGEM2-ES (orange), IPSL-CM5A-LR (purple) and MIROC5 (blue). Comparisons are shown for two European lakes (Mondsee and Würthersee), for which long-term in-situ lake surface temperatures were available. Lake temperatures are shown as annual averages (observed; black points) and with an 11-year moving average (solid lines). All temperatures are shown as anomalies relative to 1951-1980. Time series data needed to drive the lake model from each climate projection were extracted for the grid point situated closest to the centre of these lakes.

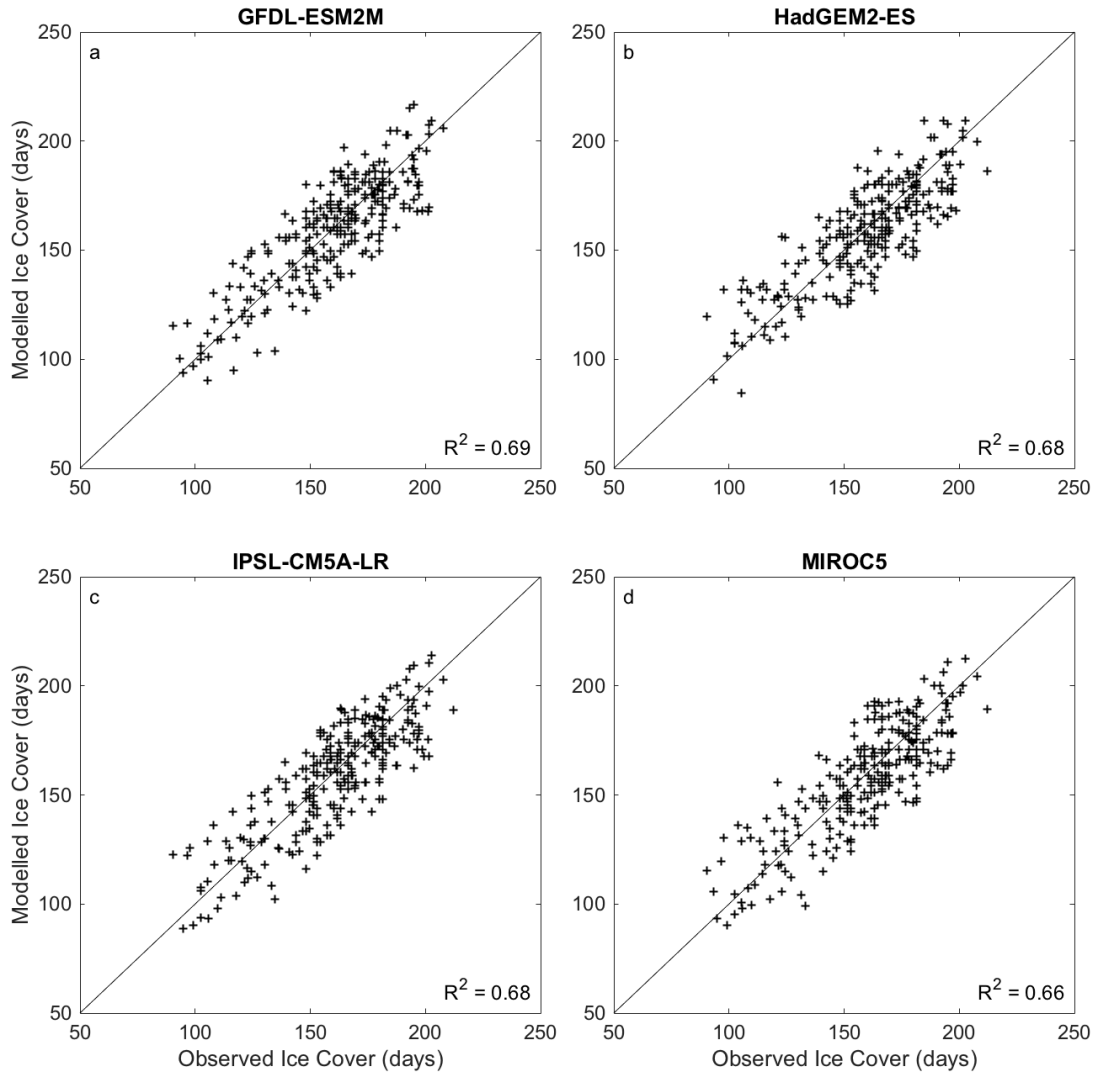


Figure S5. Comparison of modelled and observed (1995-2005) ice cover duration (in days) for the studied lakes which experienced ice cover. The modelled lake temperatures represent those simulated by a lake model forced with bias-corrected climate projections available from the Inter-Sectoral Impact Model Intercomparison Project, namely (A) GFDL-ESM2M, (B) HadGEM2-ES, (C) IPSL-CM5A-LR and (D) MIROC5. Time series data needed to drive the lake model from each climate projection were extracted for the grid point situated closest to the centre of each lake. To assess from the lake surface temperatures (observed or modelled) the period during which a lake is likely ice covered, we follow ref. 48, and characterise this as the period during which the lake-mean surface water temperature is $<1^{\circ}\text{C}$.

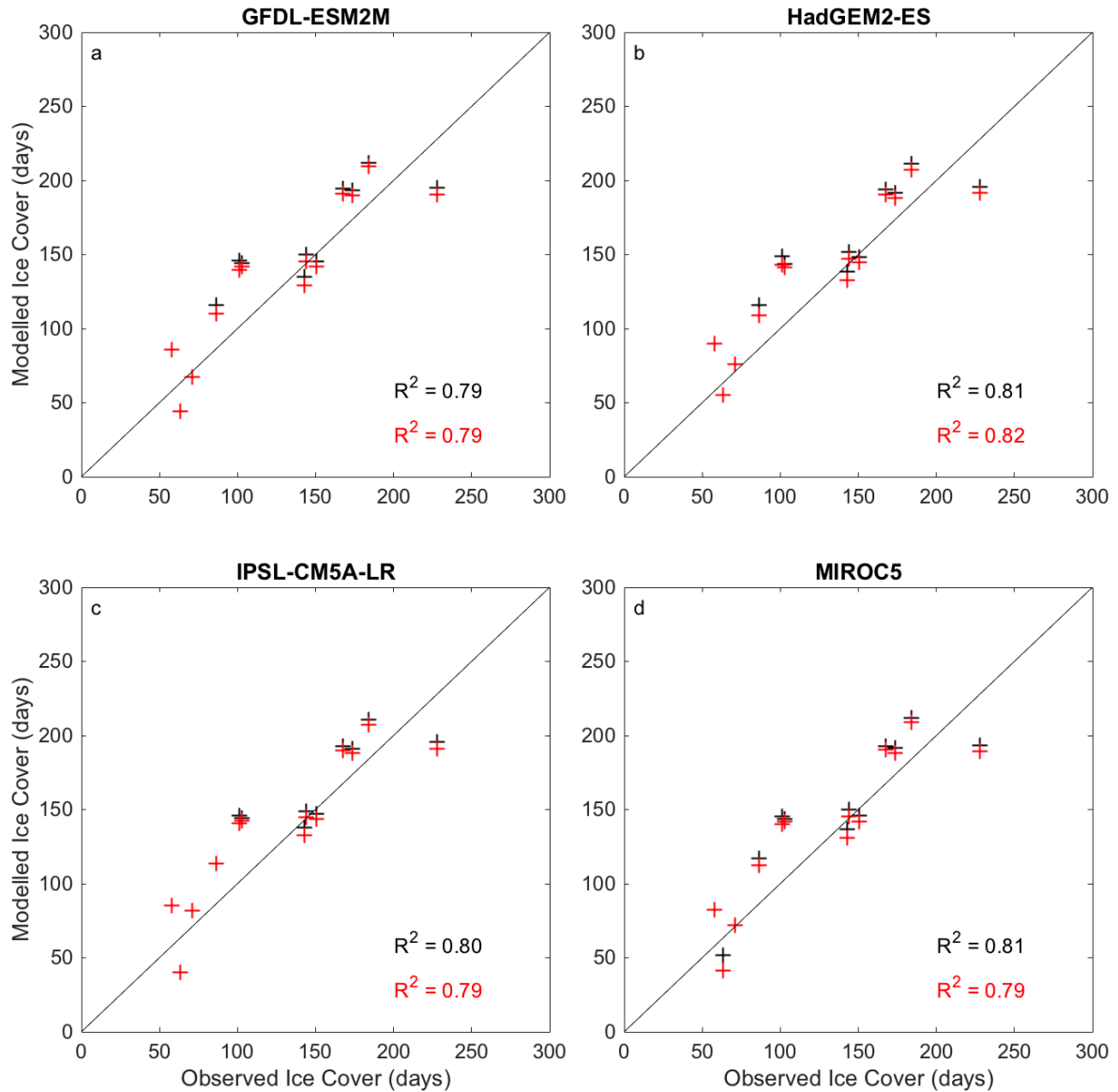


Figure S6. Comparison of modelled and observed (1995-2005) ice cover duration (in days) for lakes in which in-situ ice cover data were available and used in this study. The modelled lake temperatures represent those simulated by a lake model forced with bias-corrected climate projections available from the Inter-Sectoral Impact Model Intercomparison Project, namely (A) GFDL-ESM2M, (B) HadGEM2-ES, (C) IPSL-CM5A-LR and (D) MIROC5. Time series data needed to drive the lake model from each climate projection were extracted for the grid point situated closest to the centre of each lake. To assess from the modelled lake surface temperatures the period during which a lake is likely ice covered, we (i) follow ref. 48 and characterise this as the period during which the lake-mean surface water temperature is $<1^{\circ}\text{C}$ (black), and (ii) use the simulated period of non-zero ice thickness from the lake model (red). Observed ice cover data are from the Global Lake and River Ice Phenology Database⁶². Note that the average period of ice cover calculated for each lake will be based on a different time period, depending on the years in which observed ice cover data were available. Specifically, for some lakes only a few years of data are available, and thus the average observed ice cover duration will be different to that calculated using a 20-year period (e.g., Fig. S5).

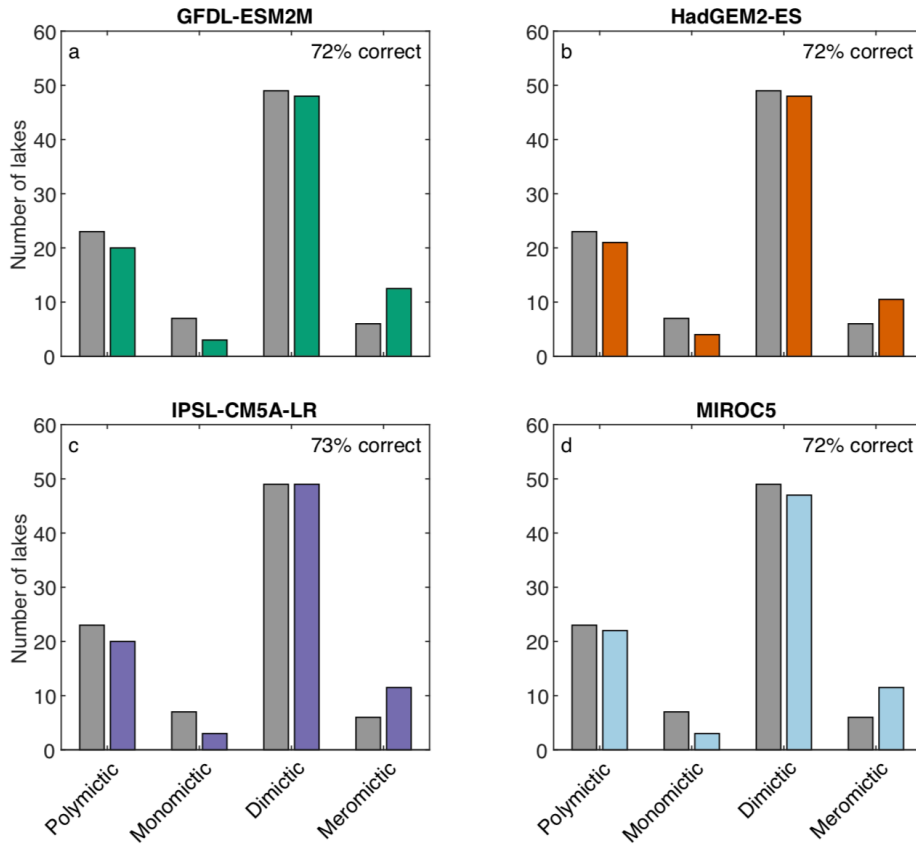


Figure S7. Comparison of modelled (grey) and literature defined (colour) mixing regimes of 85 lakes (Table S2). Modelled mixing regime classifications were defined following the method described in Fig. S1. Depth-resolved lake temperatures used in the lake mixing regime classification method were simulated by a lake model forced with bias-corrected climate projections available from the Inter-Sectoral Impact Model Intercomparison Project, namely (A) GFDL-ESM2M, (B) HadGEM2-ES, (C) IPSL-CM5A-LR and (D) MIROC5. Time series data needed to drive the lake model from each climate projection were extracted for the grid point situated closest to the centre of each lake. For each climate model projection, we also show (see inset) the percentage of correctly defined mixing regimes by the lake model driven by each of the bias-corrected climate model projections.

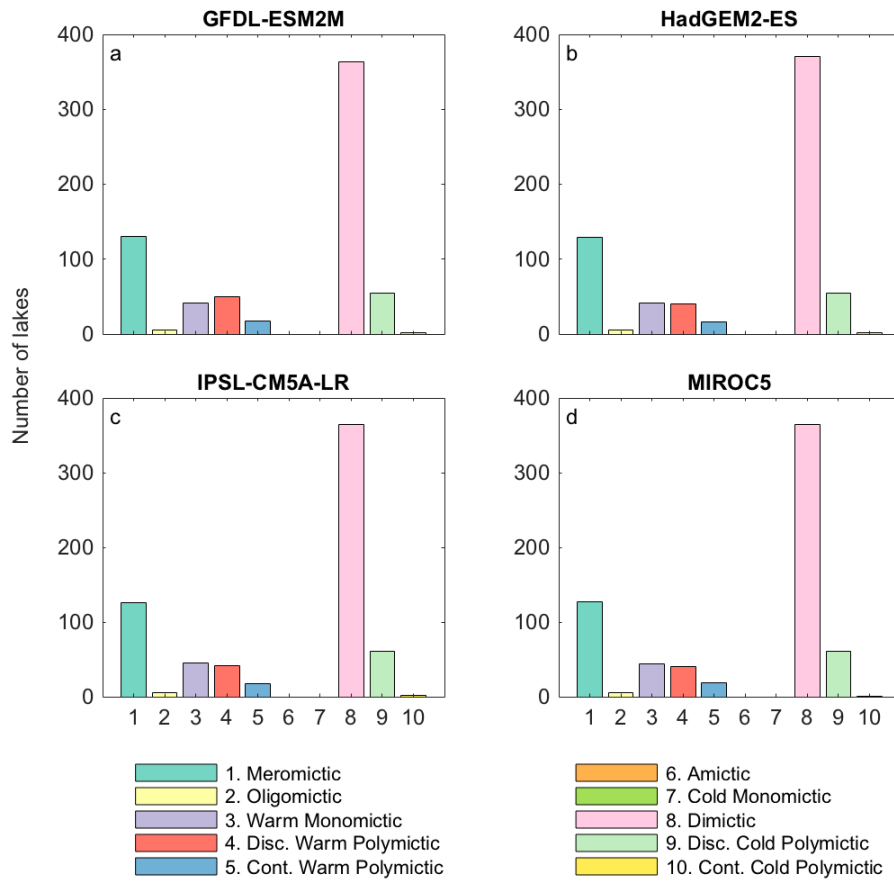


Figure S8. Comparison of modelled global lake mixing regimes identified using the classification scheme of ref. 16 and depth-resolved lake temperatures simulated by a lake model forced with bias-corrected climate projections, namely (A) GFDL-ESM2M, (B) HadGEM2-ES, (C) IPSL-CM5A-LR and (D) MIROC5.

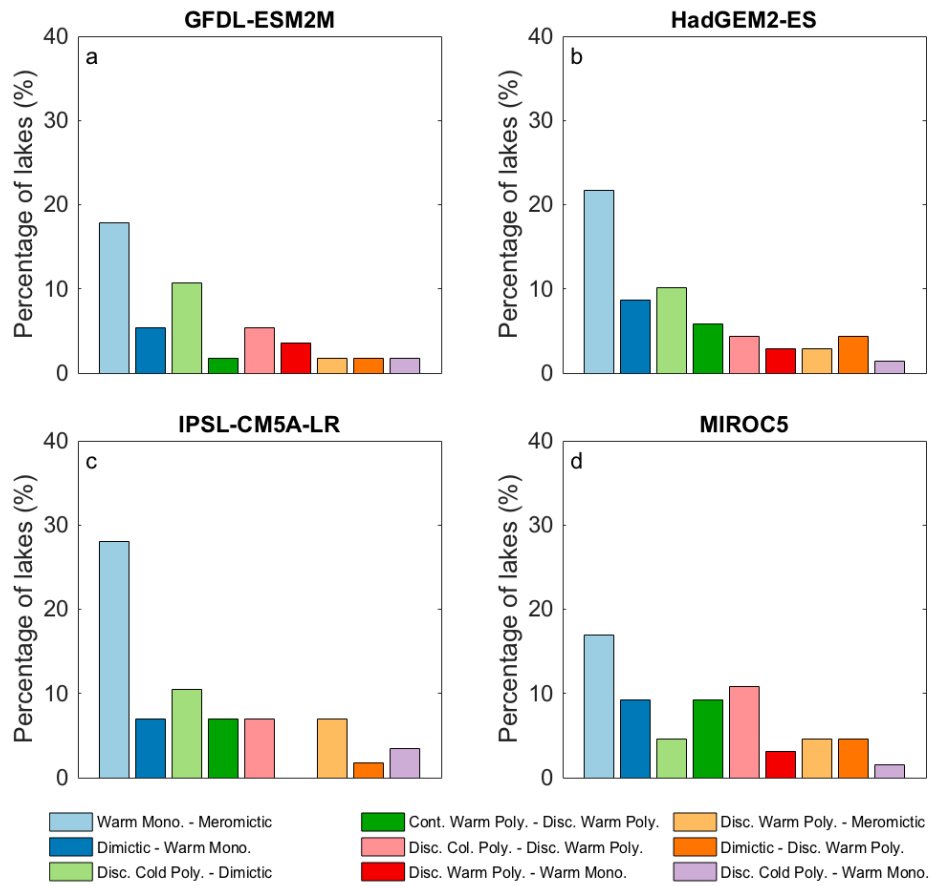


Figure S9. Comparison of climate-related changes in lake mixing regimes under RCP 2.6 using a lake model forced with bias-corrected climate projections, namely (A) GFDL-ESM2M, (B) HadGEM2-ES, (C) IPSL-CM5A-LR and (D) MIROC5.

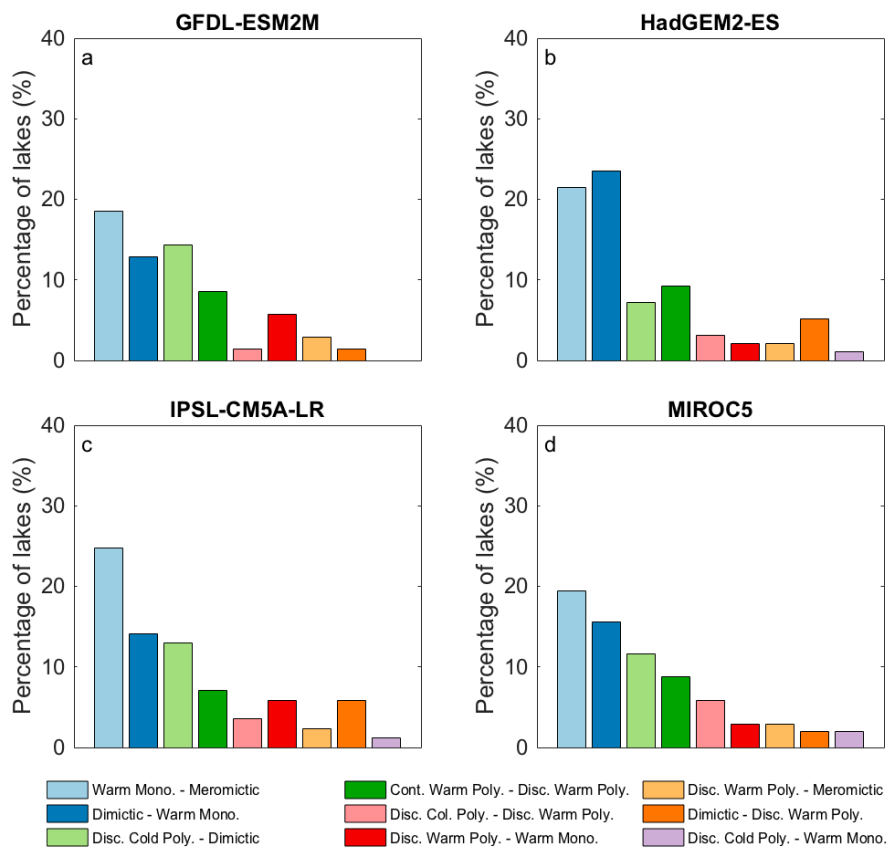


Figure S10. Comparison of climate-related changes in lake mixing regimes under RCP 6.0 using a lake model forced with bias-corrected climate projections, namely (A) GFDL-ESM2M, (B) HadGEM2-ES, (C) IPSL-CM5A-LR and (D) MIROC5.